Electro-optic detection of THz radiation in $LiTaO_3$, $LiNbO_3$ and ZnTe

C. Winnewisser,[a] P. Uhd Jepsen, M. Schall, V. Schyja, and H. Helm
Fakultät für Physik, Albert-Ludwigs-Universität, D-79104 Freiburg, Germany

(Received 6 January 1997; accepted for publication 10 April 1997)

Freely propagating THz pulses are detected in electro-optic (eo) crystals by monitoring the phase retardation (PR) of an infrared femtosecond probe pulse. This technique permits the determination of the temporal shape of the THz pulse in the subpicosecond time domain. We present measurements in $LiTaO_3$, $LiNbO_3$, and ZnTe and compare their signal performance as eo crystals with theoretical calculations for the PR signal. ZnTe shows the best performance for eo detection.
 [S0003-6951(97)01523-4]

A variety of techniques for the detection of freely propagating electro-magnetic pulses in the subpicosecond time domain, so-called terahertz (THz) pulses, have been developed. These include the method of optically gated photoconductive antennas,[1] interferometric techniques with helium cooled bolometers,[2] pyroelectric detectors,[3] and electro-optic (eo) detection.[4–7]

The motivation for eo detection of THz pulses is based on the advantage of a nearly flat frequency response (low dispersion) for certain eo-sensor crystals in the far-infrared region.[8,9] Furthermore the eo detection promises the possibility of spatially resolved THz imaging without the need to spatially scan the object. This technique was proposed recently[5,6] and as a first step Wu *et al.* succeeded in detecting the spatial profile of a THz beam.[7]

Pioneering experiments on eo sampling inside $LiTaO_3$ and $LiNbO_3$ crystals have been carried out by Auston *et al.* and Valdmanis *et al.*[10,11] Work concerning eo detection of freely propagating THz pulses has been reported only recently.[4,5,12] Our previous work[6,12] has been concerned with eo detection using $LiTaO_3$ as a sensor eo crystal and the derivation of a formula for the phase retardation (PR) induced in a copropagating probe pulse. In the present letter we have extended our earlier studies to $LiNbO_3$ and ZnTe as eo-sampling crystals. For experimental details the reader is referred to Ref. 6.

The eo detection of the THz pulses is based on the linear eo effect (Pockels effect). The electric THz field strength modifies the refractive index ellipsoid of the eo crystal. Thus the index of refraction n_i becomes $n_i = n_i(E_{\mathrm{THz}})$, where i represents one of the principal axes x,y,z. If the THz beam propagates along the z direction different phase shifts, ϕ_x and ϕ_y, result for the electric field components of the electric field strength E_x and E_y of an optical probe beam, which also propagates along the z direction. The differential PR experienced by the probe beam due to the THz field over a distance dz is denoted by $\delta\phi = \phi_y - \phi_x$.

Of the three crystals studied here $LiTaO_3$ and $LiNbO_3$ are uniaxial crystals. We also investigated ZnTe $\langle 110 \rangle$ which is an isotropic crystal with zinc blende structure.

In Figure 1 the different orientations of the eo crystals relative to the E_{THz} polarisation are illustrated. The actual PR due to the THz field depends on the crystal orientation:

(i) b-cut case: The differential PR is given by[13]:

$$\delta\phi_{\mathrm{THz}}(T) = \frac{1}{2}\frac{\omega}{c}(n_o^3 r_{13} - n_e^3 r_{33}) E_{\mathrm{THz}}(T)\cdot dz = C_b E_{\mathrm{THz}}(T)\cdot dz, \quad (1)$$

where T is the relative time delay betweeen the THz pulse and the probe pulse, r_{13} and r_{33} are components of the electro-optic tensor, C_b is a constant appropriate for the b-cut crystal orientation, and ω is the optical probe beam frequency. There is an additional, static PR term due to the natural birefringence of the b-cut crystal of

$$\delta\phi_{nat} = \frac{\omega}{c}(n_e - n_o)dz, \quad (2)$$

which gives a background signal, which cannot be cancelled by orientation of the crossed polarizers.

(ii) c-cut case: The differential PR may be written as:

$$\delta\phi_{\mathrm{THz}}(T) = \frac{\omega}{c} n_o^3 r_{22} E_{\mathrm{THz}}(T)\cdot dz = C_c E_{\mathrm{THz}}(T)\cdot dz. \quad (3)$$

In the case of a c-cut crystal the probe beam does not suffer a static PR, but has a smaller C-factor and therefore a smaller overall PR magnitude $\delta\phi_{\mathrm{THz}}$.

(iii) ZnTe $\langle 110 \rangle$ cut: In this case no intrinsic PR occurs in the crystal and the differential PR due to the THz field strength may be written as

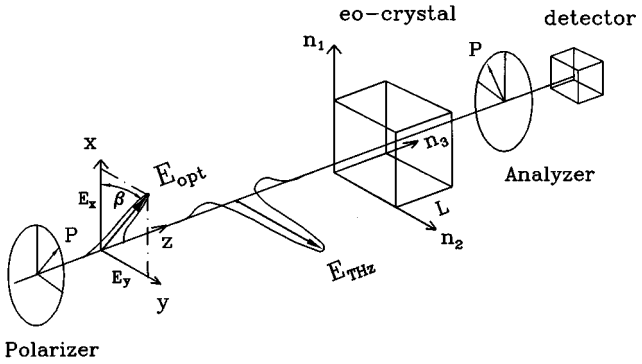

FIG. 1. eo detection setup. The optical probe pulse and the THz pulse propagate along the z axis. The optical probe beam is linearly polarized at $\beta = 45°$ and the THz field strength E_{THz} is parallel to the y axis. For b-cut crystals the following conditions hold: $n_o = n_1 = n_3$ and $n_e = n_2$. For a c-cut crystal: $n_o = n_1 = n_2$ and $n_e = n_3$.

[a]Electronic mail: winnewis@frhe20.physik.uni-freiburg.de

$$\delta\phi_{\mathrm{THz}}(T)=\frac{\omega}{c}n_o^3 r_{41}E_{\mathrm{THz}}(T)\cdot dz=C_{\mathrm{ZnTe}}E_{\mathrm{THz}}(T)\cdot dz. \tag{4}$$

In general the optical probe beam ($\lambda=800$ nm) overtakes the THz pulse inside the eo crystal, since the group velocity of the optical probe beam is greater than the THz beam by a factor of n_{THz}/n_{opt}. In order to evaluate the total PR signal, one needs to account for temporarily varying spatial overlap of the probe and the THz pulse when integrating over the crystal length L. The PR $\Delta\phi_{\mathrm{THz}}$ encountered by the optical probe pulse thus becomes[6]

$$\Delta\phi_{\mathrm{THz}}(T)=(1-R)\cdot C\int_0^L E_{\mathrm{THz}}\left(\frac{z}{c}\Delta n+T\right)e^{-\alpha z}\,dz. \tag{5}$$

The integral over the electric field strength E_{THz} of the THz beam accounts for a situation where the THz beam is attenuated inside the crystal (field absorption coefficient α) and where the probe pulse propagates with a group velocity through the crystal which is different from that of the THz pulse ($\Delta n=n_{\mathrm{THz}}-n_{probe}$). Since $n_{probe}<n_{\mathrm{THz}}$ the probe pulse effectively sweeps over the portion of the THz pulse that lies inside the crystal. All eo crystals used have a length of $L=1\ \ mm$. In order to compare our experimental data with the predictions of Eq. (5), we introduce an addional factor $(1-R)=2n_{cry}/(n_{sapph}+n_{cry})$, which accounts for the reflection losses of the THz field at the interface between the truncated sapphire lens and the eo crystal. This truncated lens is used for tighter focusing of the THz radiaton.[6] The reflection losses of the interface air/truncated sapphire lens are not taken into account in Eq. (5), because we carried out the absolute measurement of the electrical field strength E_{THz} with a silicon on sapphire (SOS) detector also using the truncated sapphire lens as a focusing element.[14] The peak electrical field strength E_{THz}^{peak} was measured at the position of the eo crystal to be 2.5 kV/cm. This calibration was carried out by comparing the peak detector current from the THz pulse with the photocurrent produced by an applied static voltage across the detector gap and assuming a homogeneous electrical field across the gap.

Figure 2 compares the PR signal of the three crystals as a function of delay time T. Taking the ratio of the peak PR signals measured by ZnTe, $LiTaO_3$ and $LiNbO_3$ one finds: $1:\frac{1}{21}:\frac{1}{46}$. An absolute PR signal may be computed by using Eq. (5). Comparing the calculated peak PR signal for ZnTe, $LiTaO_3$ and $LiNbO_3$ we determinate the ratios: $1:\frac{1}{18}:\frac{1}{43}$, which are in good agreement with the measurement. b-cut $LiTaO_3$ in comparison to c-cut $LiNbO_3$ shows an intrinsically larger PR signal, in agreement with theory. However due to the natural birefringence which occurs in the case of a b-cut uniaxial crystal, the PR signal appears relative to a large background, resulting in a reduced S/N ratio.

The eo detection technique may also be used to derive the temporal variation of $E_{\mathrm{THz}}(T)$. If the attenuation coefficient α is frequency independent, one can extract the temporal shape of the THz pulse directly from the measured phase change $\Delta\phi_{\mathrm{THz}}(T)$ by differentiating Eq. (5) in time. One derives:[6]

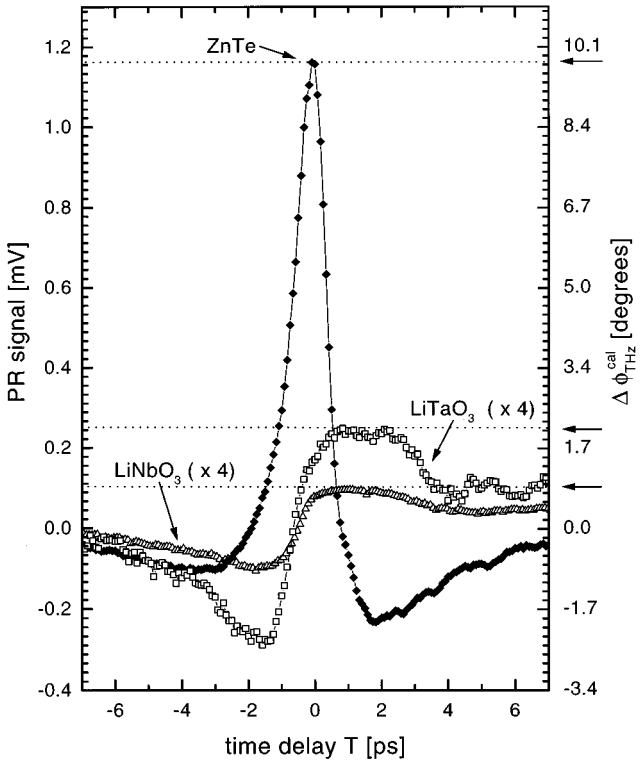

FIG. 2. The left y axis indicates PR signal measured with ZnTe (filled diamonds), b-cut $LiTaO_3$ (open squares), and c-cut $LiNbO_3$ (open triangles). The signals measured with $LiTaO_3$ and $LiNbO_3$ are multiplied by a factor of 4. The arrows on the right y axis label the values of the peak PR signals $\Delta\phi_{\mathrm{THz}}^{cal}$ calculated from Eq. (5) for different eo crystals used.

$$E_{\mathrm{THz}}(T)\propto\frac{d}{dT}\Delta\phi_{\mathrm{THz}}(T)-\frac{\alpha c}{\Delta n}\Delta\phi_{\mathrm{THz}}(T). \tag{6}$$

For small field absorption coefficients α, the second term becomes a minor correction term.

In the case of ZnTe where $\Delta n(=3.17-2.85)$ and $\alpha(=2.5\ \mathrm{cm}^{-1})$[9,15] are small, the integration of Eq. (5) reduces itself to:

$$E_{\mathrm{THz}}(T)\approx\frac{\Delta\phi_{\mathrm{THz}}(T)}{C_{\mathrm{ZnTe}}\cdot L}. \tag{7}$$

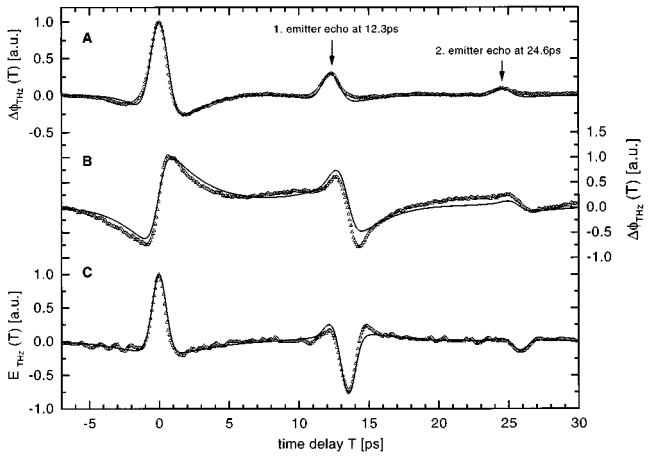

FIG. 3. Trace A: normalized PR signal measured with ZnTe. Multi étalon THz echos at $T=12.3$ ps and $T=24.6$ ps from the GaAs emitter are well resolved. The thin solid lines represent the calculated data using Eq. (5). Trace B: normalized PR signal measured with c-cut $LiNbO_3$ as sensoring crystal. Trace C: differentiated trace B giving $E_{\mathrm{THz}}(T)$.

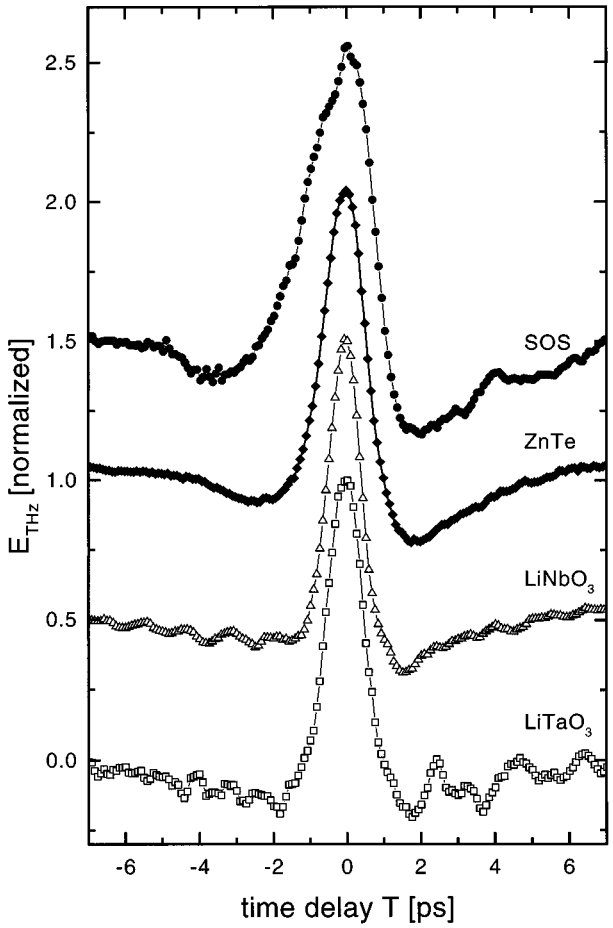

FIG. 4. The electrical THz field strength E_{THz} measured with $LiTaO_3$ (b-cut), $LiNbO_3$ (c-cut), ZnTe and with a SOS detector. The vertical zero is offset for each trace by 0.5. The SOS detector is slower compared to the eo detection mechanism, because of imperfect focusing of the optical gate pulse onto the detector gap.

In trace A of Fig. 3 the measured PR signal using ZnTe as a sensoring crystal is plotted over a longer time interval. The peaks seen at $T=12.3$ ps and $T=24.6$ ps are THz pulse etalon echoes which originate from the GaAs emitter chip. 12.3 ps corresponds to the round trip time of the THz pulse inside the GaAs slab which has a thickness of $d=520\ \mu$m.

In trace B of Fig. 3 the PR signal $\Delta\phi_{\mathrm{THz}}$ measured with $LiNbO_3$ is presented. According to Eq. (4), the temporal THz pulse shape is derived by differentiating the PR signal with respect to the time delay T, which is shown in trace C of Fig. 3. At time delay $T=0$ the THz pulse enters the $LiNbO_3$ crystal and at $T=13.6$ ps the THz pulse leaves the crystal. Since a maximum change of the PR signal is produced by the probe pulse overtaking the THz pulse as it enters or exits the eo crystal, the PR signal's derivative is positive at $T=0$ and negative at $T=13.6$ ps.

Inside the $LiNbO_3$ crystal the THz pulse suffers a small attenuation due to the field absorption coefficient of $\alpha=4$ cm^{-1},[9] attenuating the amplitude of the exiting THz pulse by the factor of $\exp(-\alpha L)$.

Furthermore a second pulse delayed by 12.3 ps is detected. This pulse is the first étalon echo from the GaAs emitter, as it also appears in the case of ZnTe. The étalon echo coincides almost in time with the signature of the THz pulse leaving the crystal at $T=13.6$ ps.

We have evaluated Eq. (5) by taking into account the multi-etalon THz echoes from the GaAs emitter and using a realistic pulse shape obtained from the first peak in trace A in Fig. 3. In traces A, B, and C of Fig. 3 the solid lines represent the calculated data for the PR measured in ZnTe and $LiNbO_3$ which are in good agreement with our experimental data.

Figure 4 shows the relative electrical THz field strength as obtained from the PR measurement. Also shown is the THz pulse measured with an SOS detector.

The small oscillations which occur in the case of b-cut $LiTaO_3$ are reproducible and are related to the static birefringence encountered by the optical probe beam.

The eo crystals $LiTaO_3$ and $LiNbO_3$ show a small S/N ratio (14:1; 28:1) due to the group velocity mismatch (GVM) between the THz pulse and the optical probe. This mismatch is reduced to a small amount in ZnTe resulting in a significantly improved S/N ratio (1000:1) as shown in Fig. 4. Wu and Zhang recently obtained a S/N ratio of 10,000:1 using a Ti:sapphire laser with an 82 MHz repetition rate.[7]

In conclusion the relative S/N performance is determined for monitoring THz pulses with ZnTe, c-cut $LiNbO_3$, and b-cut $LiTaO_3$. Measured with a 1 kHz regenerative Ti:sapphire laser the S/N ratio of the three eo crystals is about 70:2:1, respectively. Comparably low S/N ratios were obtained for c-cut $LiTaO_3$ and b-cut $LiNbO_3$ crystals. By using the measured index of refraction and the field absorption coefficients of the different crystals which were measured by THz-thermal desorption spectroscopy,[9] and using them in Eq. (5), we achieved very good agreement between theoretical and experimental data.

This research was supported by the Deutsche Forschungsgemeinschaft through Grant No. SFB 276, TP C14.

[1] P. R. Smith, D. H. Auston, and M. C. Nuss, IEEE J. Quantum Electron. **24**, 255 (1988).
[2] B. I. Greene, J. F. Federici, D. R. Dykaar, R. R. Jones, and P. H. Bucksbaum, Appl. Phys. Lett. **59**, 893 (1991).
[3] E. Budiarto, J. Marglies, S. Jeong, S. Son, and J. Bokor, IEEE J. Quantum Electron. **32**, 1839 (1996).
[4] A. Nahata, D. A. Auston, and T. F. Heinz, Appl. Phys. Lett. **68**, 150 (1996).
[5] Q. Wu and X.-C. Zhang, Appl. Phys. Lett. **67**, 3523 (1995).
[6] P. Uhd Jepsen, C. Winnewisser, M. Schall, V. Schyja, S. R. Keiding, and H. Helm, Phys. Rev. E **53**, R3052 (1996).
[7] Q. Wu, T. D. Hewitt, and X.-C. Zhang, Appl. Phys. Lett. **69**, 1026 (1996).
[8] K. P. Cheung and D. H. Auston, Infrared Phys. **26**, 23 (1985).
[9] M. Schall, C. Winnewisser, P. Uhd Jepsen, V. Schyja, and H. Helm (unpublished).
[10] D. H. Auston and A. M. Glass, Appl. Phys. Lett. **20**, 398 (1972).
[11] J. A. Valdmanis, G. Mourou, and C. W. Gabel, Appl. Phys. Lett. **41**, 211 (1982).
[12] P. Uhd Jepsen, M. Schall, V. Schyja, C. Winnewisser, S.R. Keiding, and H. Helm, *Proceedings of the Ninth International Conference on Ultrafast Processes in Spectroscopy, Trieste, Italy* Oct. 1995 (Plenum, New York, 1996), p. 654.
[13] B. E. A. Saleh and M. C. Teich, *Fundamentals of Photonics*, edited by J.W. Goodman (Wiley, New York, 1991).
[14] D. Grischkowsky, S. Keiding, M. van Exter, and Ch. Fattinger, J. Opt. Soc. Am. B **7**, 2006 (1990).
[15] S. R. Keiding (private communication).